THE EFFECTS OF SALTS ON ROAD DRYING RATES, TIRE FRICTION, AND INVISIBLE WETNESS

Thomas P. Mortimer, Pratt and Whitney, East Hartford, Conn.; and
Kenneth C. Ludema, Department of Mechanical Engineering, University of Michigan

Roads may be slippery even though they are not visibly wet. Water films of invisible thickness cause substantial reductions in skid resistance on some road surfaces. This hidden wetness exists for a short time whenever surfaces are drying from the visibly wet state. Road salts slow the drying rate, which prolongs the condition of hidden wetness. Calcium chloride solutions may produce a very persistent invisible slippery film, depending on atmospheric conditions. Equations are given for predicting fluid film drying rates and the influence on skid resistance.

•TIRE FRICTION on road surfaces is usually measured in the fully wetted condition or in the "dry" condition because these two conditions are thought to represent the lower and upper extremes of tire friction. Very little attention has been given to the condition of intermediate wetness (1, 2), even though this condition is more common than fully wetted roads and may be as dangerous.

Road wetness is usually judged in a subjective manner, but sometimes attempts are made to measure the amount of liquid on the road surface. The depth or thickness of liquid on actual road surfaces varies considerably with location. On rain-wetted roads, the average liquid film thickness is typically 10^6 to 10^7 Å (1 Å = 10^{-8}cm) or 4×10^{-3} to 4×10^{-2} in. At the other extreme, clean, dry road surfaces are covered with water films whose thickness is typically 10 to 100 Å or 4×10^{-8} to 4×10^{-7} in. The latter are adsorbed films and are invisible.

This paper is a report of an investigation of tire friction on road surfaces wetted by fluid films with an average thickness less than the fully wetted thickness. It is oriented to the problem of the transition of tire friction from low to high values as the road surface dries from the very wet state. Three points are emphasized here: Whereas water films may evaporate and thin in a regular and continuous manner, tire friction increases rather abruptly in a certain range of fluid film thickness. Second, the film thickness range at which tire friction increases does not necessarily correspond with the disappearance of the observed wetness. That is, roads that appear dry do not necessarily show dry friction characteristics. Finally, it was found that salt additives on roads have a profound effect on the time and rate of transition of tire friction from low to high values and, furthermore, that salts lower the general level of tire friction below the plain water-wetted value.

The work reported here begins with a description of the method used to obtain fluid films of desired thicknesses. The film thicknesses of greatest interest are invisible and therefore difficult to measure. The method described begins with visible fluid films. After some period of water evaporation, light interference patterns, which give a good indication of film thickness, are observed. Further évaporation produces continued film thinning until an equilibrium film thickness is reached. The equilibrium thickness is a function of surface type, atmospheric temperature, relative humidity (3), and type and concentration of salt in the film. All of these factors are considered in the evaporation model developed in the next section.

Sponsored by Committee on Surface Properties-Vehicle Interaction.

EVAPORATION MODEL

In the simple evaporation model (4) the road surface is assumed to be flat and smooth and initially covered with a uniform liquid film of thickness h_o (in Å) and molar salt concentration M_o. Note that rainwater may be taken to be a salt solution of very low molar concentration. At any instant of time t (min) after the salt film has lost some water due to evaporation, the instantaneous film thickness decreases to h_f and the molar salt concentration increases to M.

Salt additives in water decrease the evaporation rate by lowering the bulk water vapor pressure of the solution P_s (in mm Hg). Figure 1a shows P_s as a function of M for NaCl and $CaCl_2$ salts. In the model, the solution temperature and air temperature are assumed equal; so the following linear approximation can be made for P_s:

$$P_s = KM + P_o \tag{1}$$

where K (mm Hg/molar) is the slope constant, which is a function of salt type and temperature T (in deg F), and P_o (mm Hg) is the saturated water vapor pressure of the air, which is also a function of T (Fig. 1b).

Assuming that the total atmospheric pressure is 760 mm Hg, we can express the evaporation of the salt solution film as

$$t = (6 \times 10^{-6}\, M_o h_o)/(0.031 + 0.0135\, V)\left((M - M_o)/[MM_oP_o(1 - H)] + \{K/[P_o(1 - H)]^2 \ln_e\}\{M_o[KM + P_o(1 - H)]\}/\{M[KM_o + P_o(1 - H)]\}\right) \tag{2}$$

where V is the horizontal wind velocity (m/sec) and H is the relative humidity of the air expressed as a fraction. Given the atmospheric conditions (i.e., T, H, and V), the salt type (i.e., K), and the initial conditions (i.e., h_o and M_o), the time t required for the solution to evaporate from salt concentration M_o to M can be calculated by using Eq. 2. Figure 2 shows families of curves for $\log_{10} M$ versus t for various initial concentrations of NaCl and $CaCl_2$ solutions with h_o = 3,000 Å at the atmospheric conditions indicated. The Xs on the NaCl solution curves denote the points at which the solutions begin to crystallize. $CaCl_2$ is deliquescent with these atmospheric conditions; these solutions therefore reach an equilibrium salt concentration instead of crystallizing.

The instantaneous salt solution film thickness can be calculated by using the expression,

$$h_f = h_o\,(M_o/M) \tag{3}$$

Figure 3 shows curves for h_f versus t corresponding to the solutions and conditions shown in Figure 2. Note that the film thinning is fairly regular and continuous. Also note that the 1.0 M_o $CaCl_2$ solution approaches an equilibrium film thickness of about 650 Å.

Given the ability to calculate fluid film thickness and molar salt concentration as a function of time, we can calculate the viscous drag force of smooth rubber sliding over smooth glass with a known fluid film between. Because we used a smooth rubber slider mounted on a British portable tester (Fig. 4) to check the model calculations, the viscous drag force was converted to units of British portable number (BPN), the average coefficient of friction multiplied by 100. The viscous drag force F was calculated by using Newton's law (5),

$$F = \eta Av/h \tag{4}$$

where

η = bulk viscosity of the salt solution film,
A = contact area,
v = relative sliding velocity, and
h = total film thickness.

Figure 1. Water vapor pressure versus (a) M and (b) T.

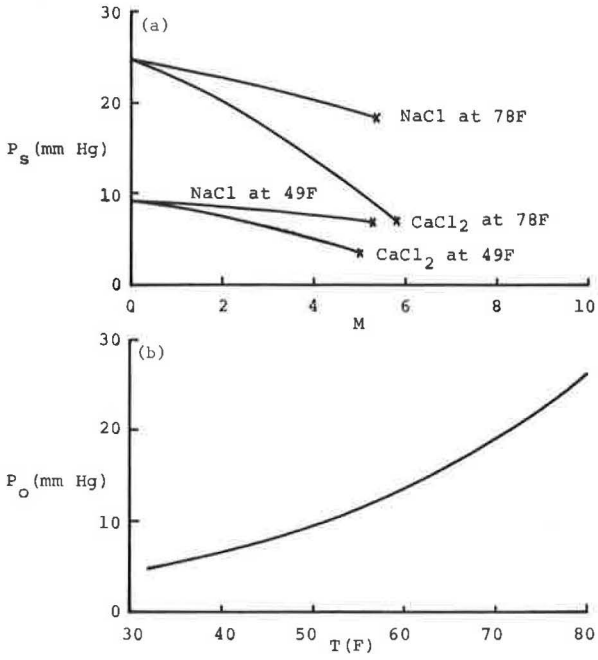

Figure 2. Evaporation model $\log_{10}M$ versus t for h_o = 3,000 Å at T = 78 F, H = 0.50, and V = 0.5 m/sec.

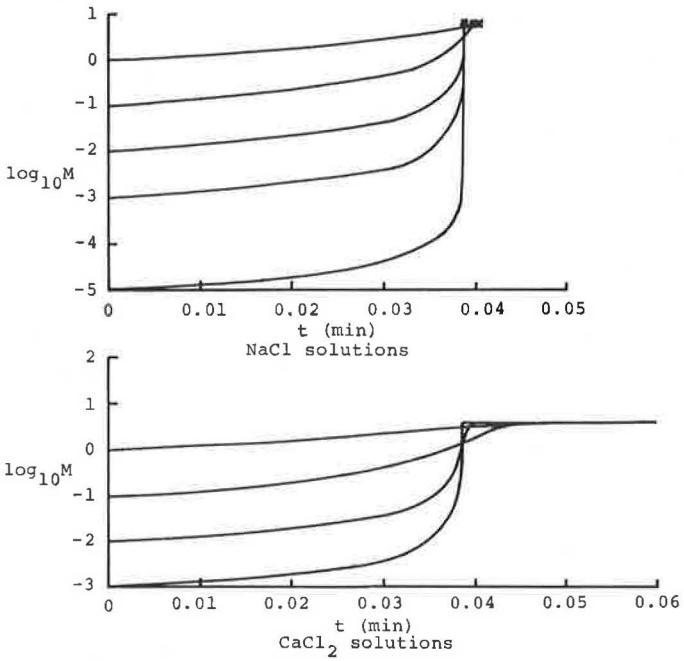

It is recognized that this simple viscous drag equation does not represent the actual case of a tire sliding over a textured road surface, but it was helpful in checking the validity of the evaporation model. The values of A and v corresponding to the British portable tester were 0.108 in.^{2} and 121 in./sec (6.9 mph). The instantaneous value of η corresponding to M was obtained from Figure 5, which shows the bulk viscosity of the salt solution divided by the bulk viscosity of pure water η/n_o as a function of M. Finally, the value of h was defined as

$$h = h_f + h_a \tag{5}$$

where h_a is the adsorbed film thickness on the clean surface. For the type of glass used in the experiments, the reference value of h_a with $\eta/n_o = 1.0$ was 89 Å at 78 F and 132 Å at 49 F.

Figures 6, 7, and 8 show the evaporation model curves of BPN versus t. The 10^{-5} M_o NaCl solutions are the approximate equivalent of distilled water. The curves in Figure 6, which correspond to those in Figures 2 and 3, show that the rate of transition of BPN is rather rapid for low initial concentrations and is more gradual for high initial concentrations. Figure 7 shows curves for 10^{-5} M_o NaCl, 1.0 M_o NaCl, and 1.0 M_o $CaCl_2$ at low and high humidity. Note that neither salt is deliquescent at low humidity, whereas both are at high humidity. The curves in Figure 7 show that, as humidity increases, the time of transition of BPN is longer and the rate of transition of BPN is less rapid. Comparison of the 1.0 M_o curves at either humidity shows that the $CaCl_2$ solution has a longer time of transition and a less rapid rate of transition than the NaCl solution. The same is true of these two salt types for any other atmospheric condition or initial concentration, but the difference is less noticeable with low humidities and initial concentrations. The difference between the 10^{-5} M_o and 1.0 M_o solutions is also less pronounced with low humidities. Figure 8 shows how temperature and wind velocity affect the transition of BPN. Note that the wind velocity affects the time and rate of transition but not the equilibrium BPN.

These evaporation model curves were checked by experiment in the following manner. A glass plate surface was first wetted with an excess of solution and then wiped with a rubber-bladed window squeegee. It was deduced that $h_o \cong 3{,}000$ Å from the fact that light interference patterns appeared almost immediately after wiping with the squeegee. The first British portable test swing was made just after wiping, and subsequent test swings were made at 0.5-min intervals without rewetting the test surface.

From a comparison of the experimental data of BPN versus t with the evaporation model curves, the following conclusions were made:

1. The evaporation model predicts correctly the relative effects on the time and time rate of transition of BPN of salt type (NaOH, NaBr, NaI, KCl, and LiCl as well as NaCl and $CaCl_2$), initial salt concentration, and atmospheric conditions.
2. The times predicted by the evaporation model are approximately 10 times faster than those that actually occur (i.e., the predicted evaporation rate is faster than the actual rate). This discrepancy is thought to be caused by four conditions not accounted for in the simple evaporation model: (a) a decrease of the liquid film temperature below air temperature due to the cooling effect of the evaporation process, (b) a salt concentration gradient in the thickness direction in which the liquid at the air surface is salt-rich, (c) a decrease of the water vapor pressure of thin films due to the absorbate surface force fields, and (d) a decrease of the water vapor pressure of thin films due to the capillary effect of a microscopically rough surface.

EVAPORATION TESTS AND TRANSITIONS IN SKID RESISTANCE AS MEASURED BY THE BRITISH PORTABLE TESTER

Evaporation tests were made on five textured road surfaces to determine if the evaporation model predicts the relative effects of salt type, salt concentration, and atmospheric conditions on the time and rate of transition of BPN on real roads as well as on glass. Pictures of the five test surfaces are shown in Figure 9. All but the Dorset pebble surface were worn under actual traffic conditions. For a

Figure 3. Evaporation model h_f versus t for h_o = 3,000 Å at T = 78 F, H = 0.50, and V = 0.5 m/sec.

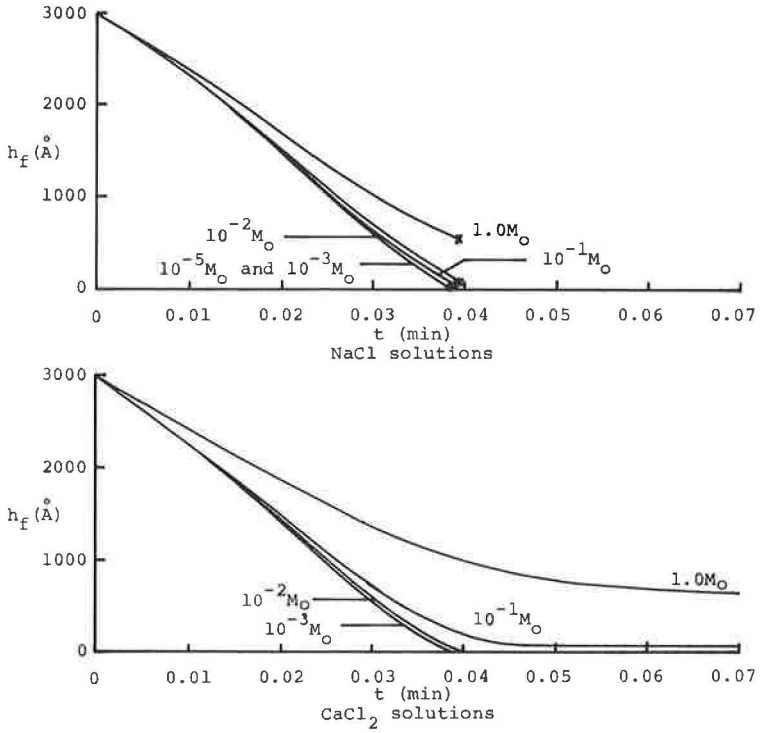

Figure 4. British portable tester.

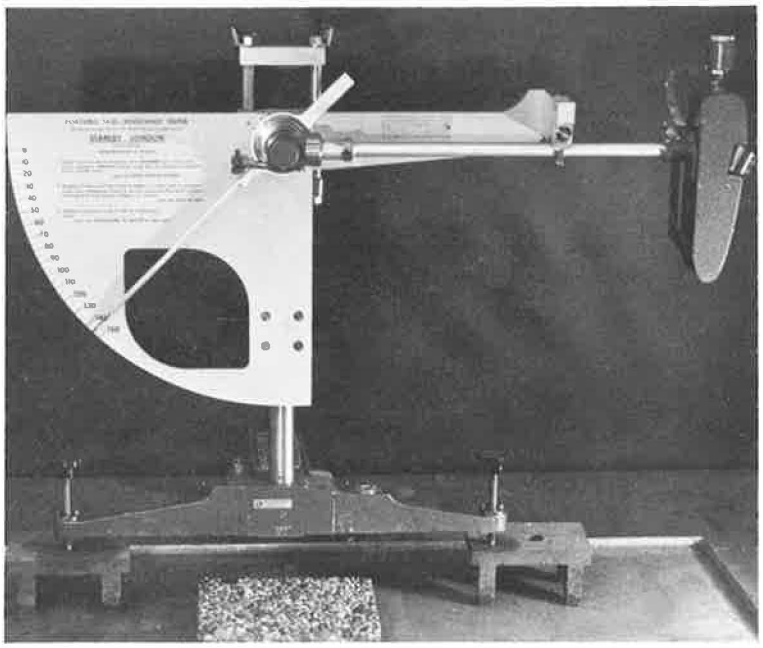

Figure 5. η/η_o **versus M (at T = 78 F,** η_o **= 0.008817 poise; at T = 49 F,** η_o **= 0.013077 poise).**

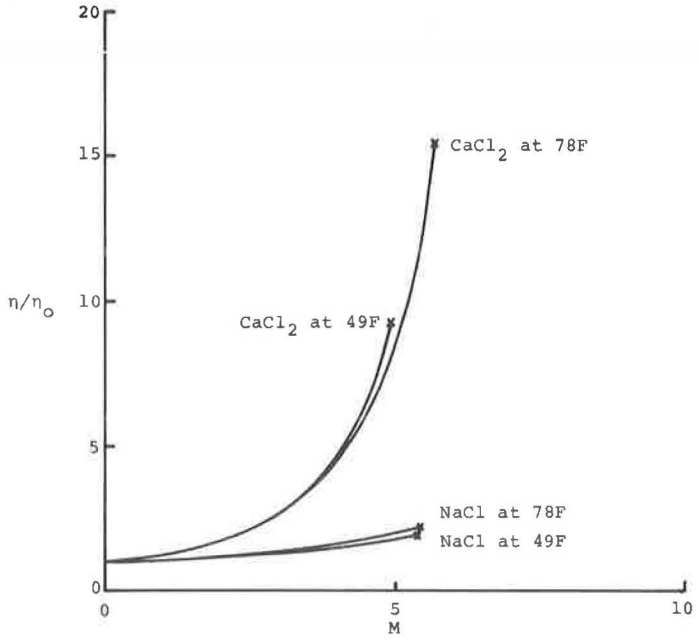

Figure 6. Evaporation model BPN versus t for h_o **= 3,000 Å at T = 78 F, H = 0.50, and V = 0.5 m/sec.**

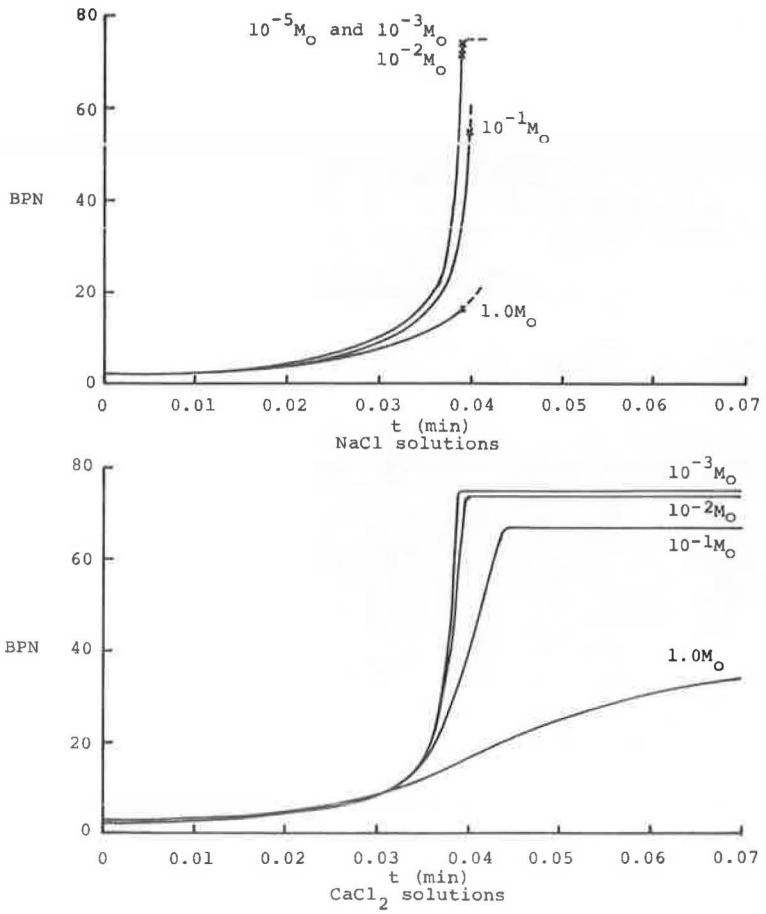

Figure 7. Evaporation model BPN versus t for h_o = 3,000 Å at T = 78 F and V = 0.5 m/sec.

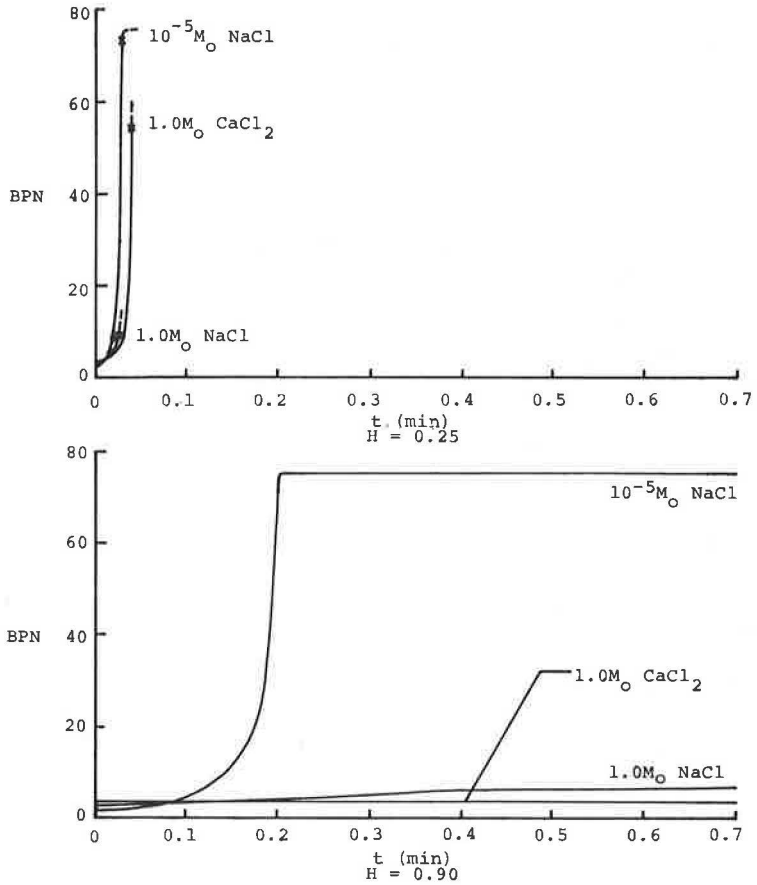

Figure 8. Evaporation model BPN versus t for h_o = 3,000 Å at T = 49 F, H = 0.62, and V = 1.0 or 0.0 m/sec.

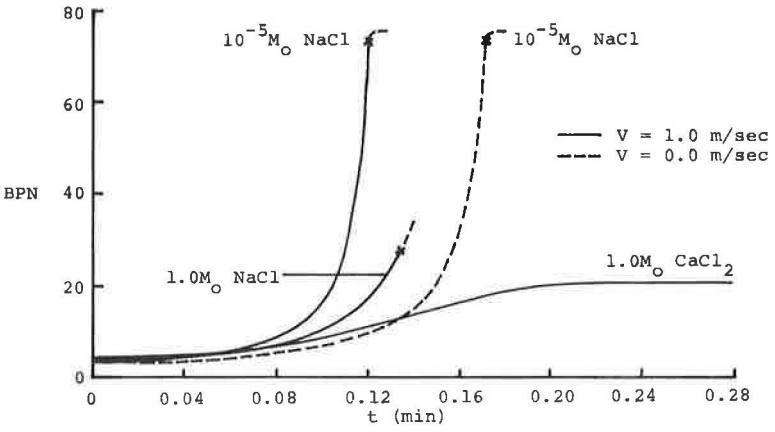

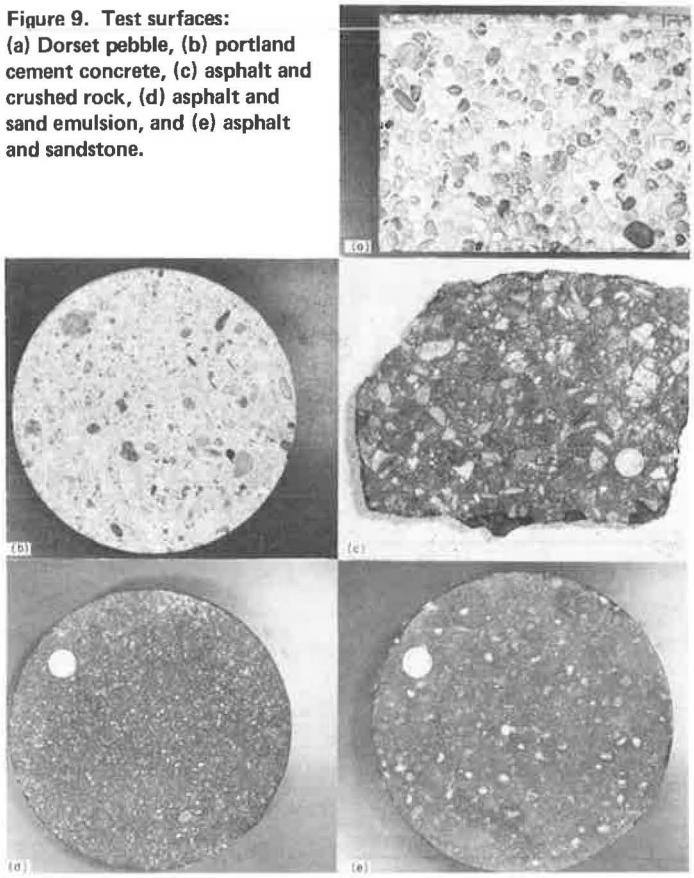

Figure 9. Test surfaces: (a) Dorset pebble, (b) portland cement concrete, (c) asphalt and crushed rock, (d) asphalt and sand emulsion, and (e) asphalt and sandstone.

Figure 10. Dorset pebble BPN versus t.

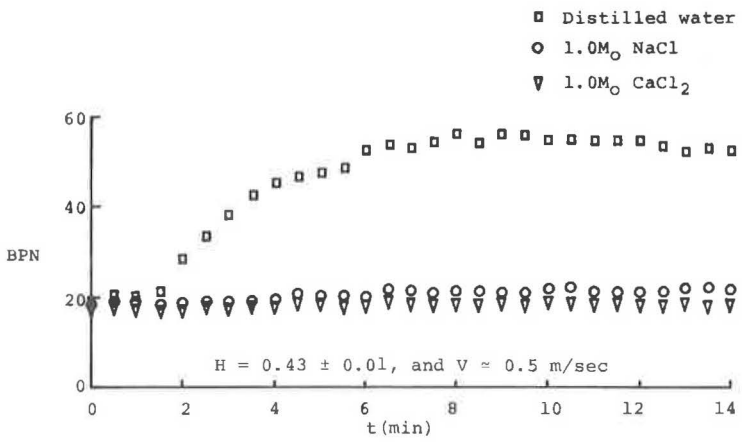

reference, the BPNs from a standard test (i.e., using distilled water, a 5-in. slide length, and a standard natural rubber slider) were measured at 78 F and are as follows: Dorset pebble, 24; portland cement concrete, 58.3; asphalt and crushed rock, 52.5; asphalt and sand emulsion, 57; and asphalt and sandstone, 62.

In the evaporation tests a slide length of 4 in. was used, and the rubber sliders were made from Royalene 505, a styrene-butadiene experimental tread stock. At the beginning of the tests, 30 ml of distilled water 1.0 M_o NaCl or 1.0 M_o $CaCl_2$ solution was spread over the clean dry test surface. The amount of salt per unit area spread on the test surface in the 1.0 M_o salt solution tests is approximately equal to that spread on road surfaces to melt ice and snow (approximately 300 to 500 pounds per lane-mile). Test swings were made without rewetting at 0.5-min intervals with the Dorset pebble surface and at 5.0-min intervals with the other road surfaces. The test data of BPN versus t are shown in Figures 10 through 14. The S and F in these figures denote the approximate start and finish of the driving of the surface as was carefully observed from directly overhead. In comparing Figures 10 through 14 with the evaporation model curves, we see that the time scales of the BPN versus t data are considerably different from the model. Part of this difference is due to the fact that the initial film thicknesses are considerably greater than 3,000 Å. Other possible causes besides the four already put forth for the glass plate tests are rewetting due to splashing from trapped liquid pools; increased liquid spreadability due to the fine scale surface texture (3); and changed air circulation patterns at the liquid surfaces, which affects the local evaporation rates. Despite this difference of the time scales, the evaporation model does predict the relative effects of salt type, initial concentration, and atmospheric conditions on the time and time rate of transition of BPN with these textured test surfaces.

EVAPORATION TESTS AND TRANSITIONS IN TIRE FRICTION AS MEASURED BY A SKID TRAILER

BPN skid resistance as usually measured on fully water-wetted roads has been shown to correlate with locked-wheel tire friction for car speeds from 20 to 50 mph (6). It was not known, however, if such a correlation exists for road surfaces of transition wetness, or film thickness, such as exist in the evaporation tests. For this reason, the validity of the findings from the evaporation tests with the British portable tester on textured surfaces was checked by performing similar evaporation tests on a real road surface and by measuring tire friction directly with the two-wheeled skid trailer (ASTM Standard E 274-65T) of the Michigan Department of State Highways. The skid trailer tires (ASTM Standard E 249-66) had a vertical load of approximately 800 lb each. Pictures of the test vehicle and the trailer tire are shown in Figures 15 and 16. The test site chosen was the outer lane of a uniform, level stretch of a 15-year-old portland cement concrete divided highway in southern Michigan. The road surface is similar in appearance to the test surface shown in Figure 9b. For a reference, the BPN from a standard test on this road surface at 47 F was 59.8.

In these evaporation tests, the test lane was blocked off to traffic, and three separate 60- by 10-ft sections were wetted, one with 15 gal of tap water, one with 1.0 M_o NaCl solution, and one with 1.0 M_o $CaCl_2$ solution. The volume of solution per unit area spread on the road surface was approximately the same as that used in the evaporation tests. The average coefficient of tire friction μ in full skidding at 40 mph of the three wetted test sections was periodically measured. To minimize the contamination of one solution by the others required that the skid trailer wheels be washed between each test run. Throughout the test the sky was overcast, and the atmospheric conditions remained nearly constant. Figure 17 shows μ as a function of t, which is the total elapsed time since the solution in that section was first tested.

It is seen from the curves that the relative times and time rates of transition of μ are in agreement with the transitions of BPN in the other evaporation tests and with the evaporation model. Because the evaporation model is based on viscous drag, the test data suggest that fluid viscous effects are prominent in tire friction in the transition film thickness range.

The skid trailer data confirmed the findings of British portable tests, which showed that salt additives decrease the general level of friction in the fully wetted condition.

Figure 11. Portland cement concrete BPN versus t.

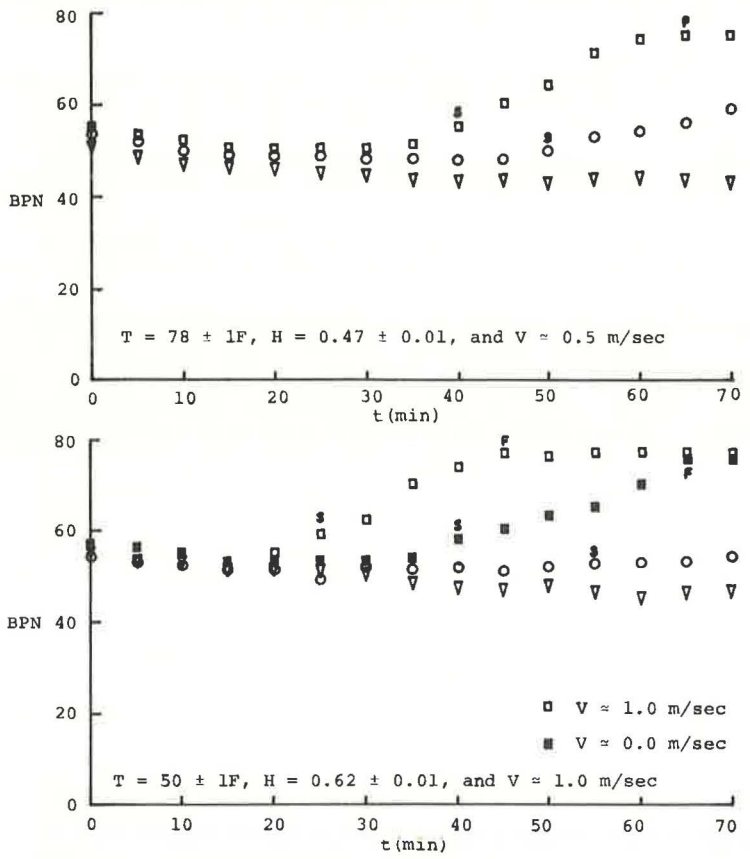

Figure 12. Asphalt and crushed rock BPN versus t.

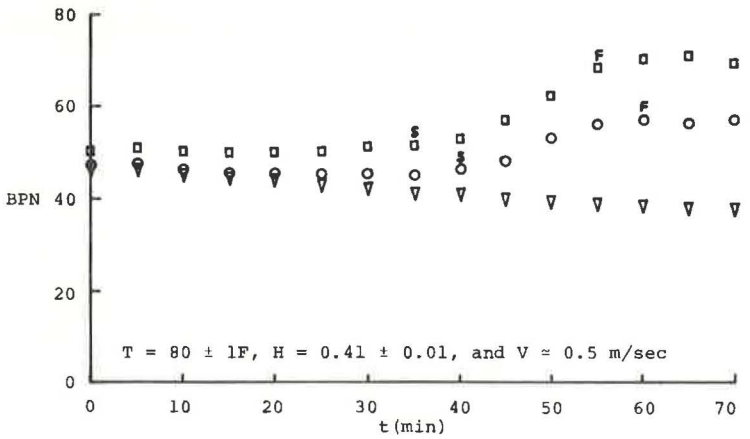

Figure 13. Asphalt and sand emulsion BPN versus t.

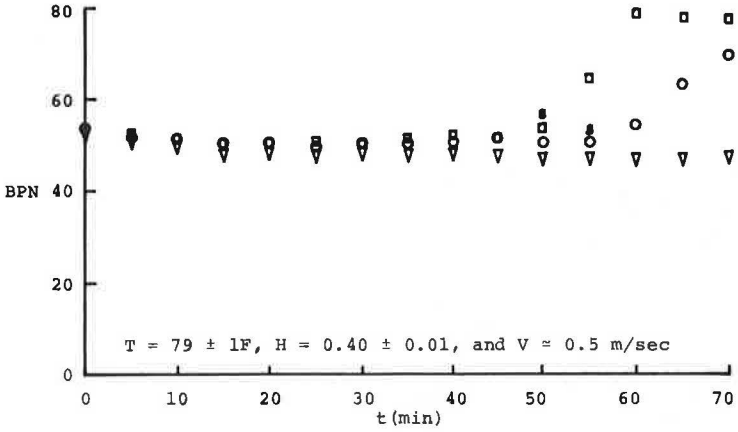

Figure 14. Asphalt and sandstone BPN versus t.

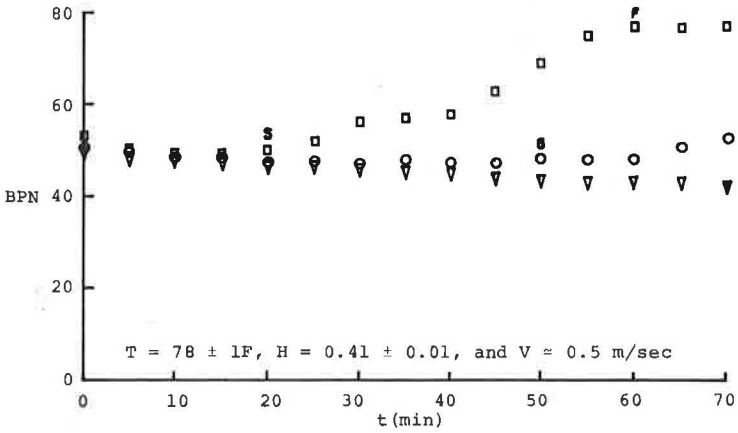

Figure 15. Test vehicle.

Figure 16. Trailer tire.

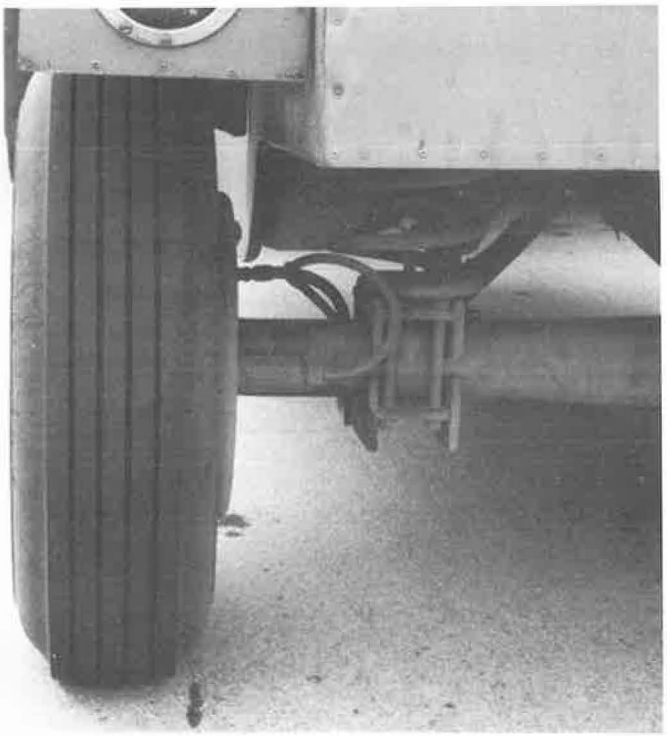

Figure 17. Portland cement concrete μ versus t.

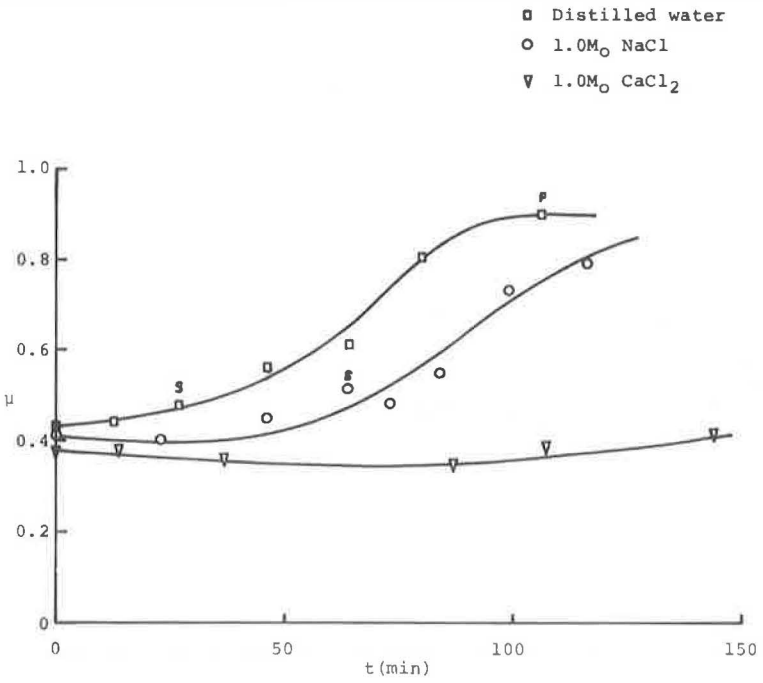

The probable reason is that the squeeze film between the tire and road surface is thicker for the salt solutions because they have a bulk viscosity greater than pure water (Fig. 5). Csathy (2) tested real road surfaces with a British portable tester and reported a BPN decrease of 7 to 10 percent with 4.65 M NaCl solution and 12 to 15 percent with 2.5 M $CaCl_2$ solution. A BPN decrease of similar magnitude was observed in the evaporation tests reported in this paper. The skid trailer tire friction data showed an initial decrease of 4.7 percent for 1.0 M_o NaCl solution and 11.6 percent for 1.0 M_o $CaCl_2$ solution. After some evaporation had taken place and the bulk viscosity of the salt solution had increased, the value of μ with the salt solutions reached a minimum, and the decrease below the plain water-wetted value was 7.0 percent for the NaCl solution and 18.6 percent for the $CaCl_2$ solution.

INVISIBLE WETNESS

In the evaporation tests on the glass plate surface, the liquid films were directly visible at first, then interference fringes were seen, and after this no evidence of water was apparent. The minimum light interference film depth was calculated to be approximately 1,700 Å (4). Thinner films were invisible, and yet the BPN value continued to increase with time just as predicted by the evaporation model. The BPN value when the glass plate first appeared dry was approximately 30. In contrast, the maximum dry value for the clean plate was over 84. The condition in which a surface appears dry but has a friction value significantly below the clean, dry value is termed "invisible wetness." The evaporation test data on the glass plate showed that one of the effects of salt additives in solution is to temporarily or indefinitely delay the decrease in film thickness and the increase in BPN, i.e., to prolong the condition of invisible wetness.

Invisible wetness poses a problem for drivers who mistakenly perceive a road surface to be dry when in fact the actual tire friction is significantly below the expected clean, dry level. In the evaporation experiments on the textured road surfaces, there was some evidence that under certain conditions invisible wetness does in fact occur. For the Dorset pebble and portland cement concrete road surfaces, which have porous cement binders and nonporous road stone aggregates, the driver usually determines road wetness from the cement binder appearance. The road is perceived to be dry when the binder is light and wet when dark. Evaporation tests with the British portable tester showed, however, that the matrix does not always reveal the true wetness. For example, in evaporation tests with 10^{-1} M_o $CaCl_2$ solutions, the porous cement binder absorbed the solution after 15 to 30 min and began to appear light, which is characteristic of a dry surface. The nonporous road stones over which the rubber surface slides maintained relatively thick but invisible liquid films, however. In this condition of invisible wetness, the Dorset pebble BPN was about 35 compared to the dry upper limit of 85, and the portland cement concrete BPN was about 65 compared to the dry upper limit of 75.

The asphalt binder of the three asphalt surfaces was much darker than the cement binder, and the change in darkness from the wet to the dry condition was much less pronounced than with the cement binder. The asphalt matrix tended to be less porous, however, which kept the matrix wet longer and helped to offset the difficulty in detecting the binder wetness. The degree of danger from invisible wetness with the asphalt road surfaces is about the same as that with the portland cement concrete surface.

CONCLUSIONS

Salt additives in the solution wetting a road surface have the effect to temporarily or indefinitely delaying the drying of the surface and thereby delaying the transition of tire friction from the wet to the dry value. The evaporation model described in this paper predicts the relative effects on the transitions of tire friction of salt type, salt concentration, and atmospheric conditions. Three significant effects are as follows:

1. $CaCl_2$ delays the transition more than the equivalent molar concentration of NaCl and is therefore a more undesirable road contaminant in terms of tire friction.
2. The greater the concentration of a particular salt type is, the slower is the transition from the wet to the dry friction level.

3. The higher the air humidity is, the greater is the effect that salt contaminants have in prolonging the transition from the wet to the dry friction level.

Salt contaminants in the solution wetting road surfaces can decrease tire friction below the uncontaminated water-wetted value. This decrease is as large as 7.0 percent for NaCl and 18.6 percent for $CaCl_2$. Also, salt contaminants on road surfaces increase the equilibrium film thickness and thereby promote the condition of invisible wetness in which the road surface appears dry but in fact has a level of tire friction significantly below the clean, dry value.

ACKNOWLEDGMENTS

We thank David Sapper of the Uniroyal Tire Company, Detroit, Michigan, for supplying the Royalene 505 rubber used in the experiments.

REFERENCES

1. Moyer, R. A. Skidding Characteristics of Road Surfaces. HRB Proc., Vol.13, Pt. 1, 1934, pp. 123-168.
2. Csathy, T. I. A Study of the Skid-Resistance of Pavement Surfaces. Department of Highways, Ontario, DHO Rept. 32, 1963, pp. 9-14.
3. Holland, L. The Properties of Glass Surfaces. Chapman and Hall, London, 1964, pp. 227, 349-351.
4. Mortimer, T. P. The Effects of Ions in Aqueous Solution on Wet Rubber Friction. PhD thesis, Univ. of Michigan, 1971, pp. 118-130, 141-143.
5. Hersey, M. D. Theory and Research in Lubrication. John Wiley and Sons, New York, 1966, p.26.
6. Mahone, D. C. Pavement Friction as Measured by the British Portable Tester and by the Stopping-Distance Method. Materials Research and Standards, Vol. 2, No. 3, March 1962.